Cell Reports

GRP94 Regulates Circulating Cholesterol Levels through Blockade of PCSK9-Induced LDLR Degradation

Graphical Abstract

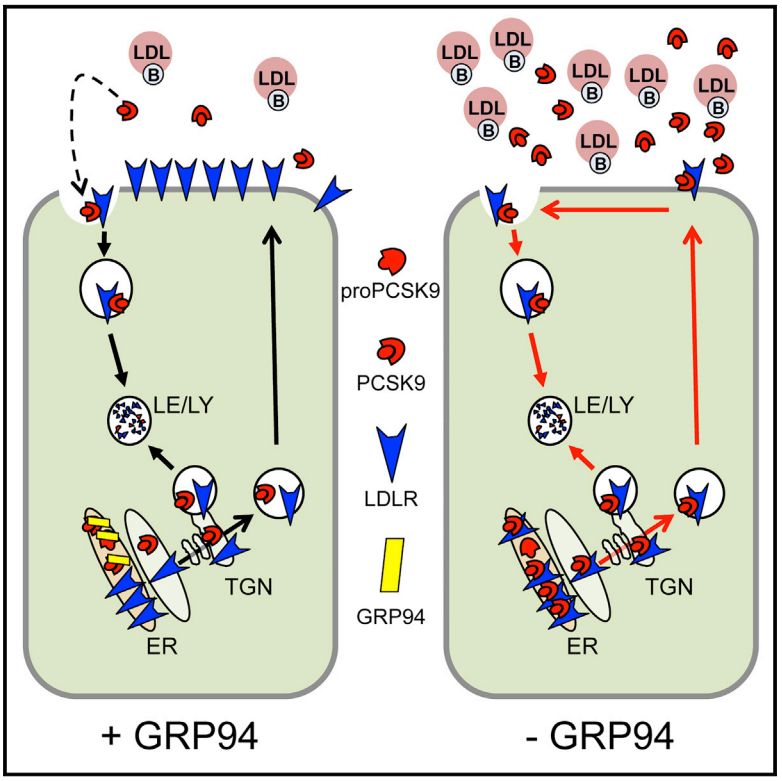

Authors

Steve Poirier, Maya Mamarbachi, Wan-Ting Chen, Amy S. Lee, Gaetan Mayer

Correspondence

gaetan.mayer@icm-mhi.org

In Brief

Clearance of circulating LDL cholesterol depends primarily on hepatic LDL receptor (LDLR). Poirier et al. show that the ER-resident chaperone GRP94 interacts and inhibits PCSK9, a natural inducer of LDLR degradation. By preventing PCSK9 binding to LDLR, GRP94 regulates circulating LDL by maintaining LDLR protein levels in hepatocytes.

Highlights

- PCSK9 interacts with the ER-resident chaperone GRP94
- GRP94 is not an obligatory chaperone for PCSK9
- In the absence of GRP94, LDLR is more sensitive to PCSK9-mediated degradation
- GRP94 regulates LDLc levels by maintaining LDLR protein levels

Poirier et al., 2015, Cell Reports *13*, 2064–2071
December 15, 2015 ©2015 The Authors
http://dx.doi.org/10.1016/j.celrep.2015.11.006

CellPress

OPEN ACCESS
CellPress

Cell Reports
Report

GRP94 Regulates Circulating Cholesterol Levels through Blockade of PCSK9-Induced LDLR Degradation

Steve Poirier,[1,2] Maya Mamarbachi,[1] Wan-Ting Chen,[3] Amy S. Lee,[3] and Gaetan Mayer[1,2,4,*]
[1]Laboratory of Molecular Cell Biology, Montreal Heart Institute, Montréal, QC H1T 1C8, Canada
[2]Department of Pharmacology, Faculty of Medicine, Université de Montréal, Montréal, QC H3C 3J7, Canada
[3]Department of Biochemistry and Molecular Biology, Keck School of Medicine, USC Norris Comprehensive Cancer Center, University of Southern California, Los Angeles, CA 90089-9176, USA
[4]Department of Medicine, Faculty of Medicine, Université de Montréal, Montréal, QC H3C 3J7, Canada
*Correspondence: gaetan.mayer@icm-mhi.org
http://dx.doi.org/10.1016/j.celrep.2015.11.006

SUMMARY

Clearance of circulating low-density lipoprotein cholesterol (LDLc) by hepatic LDL receptors (LDLR) is central for vascular health. Secreted by hepatocytes, PCSK9 induces the degradation of LDLR, resulting in higher plasma LDLc levels. Still, it remains unknown why LDLR and PCSK9 co-exist within the secretory pathway of hepatocytes without leading to complete degradation of LDLR. Herein, we identified the ER-resident GRP94, and more precisely its client-binding C-terminal domain, as a PCSK9-LDLR inhibitory binding protein. Depletion of GRP94 did not affect calcium homeostasis, induce ER stress, nor did it alter PCSK9 processing or its secretion but greatly increased its capacity to induce LDLR degradation. Accordingly, we found that hepatocyte-specific *Grp94*-deficient mice have higher plasma LDLc levels correlated with ~80% reduction in hepatic LDLR protein levels. Thus, we provide evidence that, in physiological conditions, binding of PCSK9 to GRP94 protects LDLR from degradation likely by preventing early binding of PCSK9 to LDLR within the ER.

INTRODUCTION

Familial hypercholesterolemia is a common genetic disorder affecting ~1 in 200–500 people that inherit genetic mutations mostly in low-density lipoprotein (LDL) receptor (*LDLR*), apolipoprotein B-100 (*APOB*), or proprotein convertase subtilisin kexin type 9 (*PCSK9*) loci (Nordestgaard et al., 2013). *PCSK9* encodes for a natural inducer of LDLR degradation (Maxwell and Breslow, 2004), for which patients harboring gain-of-function mutations have high levels of circulating LDLc (Abifadel et al., 2003). Conversely, *PCSK9* loss-of-function mutations (Cohen et al., 2005) or pharmacological inhibition significantly increase clearance of plasma LDL particles by hepatocytes (reviewed in Poirier and Mayer, 2013). Therefore, PCSK9 represents an emerging lipid-lowering therapeutic target to reduce progression of atherosclerosis and risk of coronary heart diseases (CHDs).

PCSK9 is a sterol-regulated gene mainly expressed in liver and to a lesser extent in kidney and intestine (Maxwell et al., 2003; Seidah et al., 2003). Within the ER, PCSK9 is autocatalytically cleaved (Seidah et al., 2003), resulting in a tightly bound secretable heterodimeric complex (Cunningham et al., 2007). Following binding with PCSK9 (McNutt et al., 2007), LDLR is rerouted from the cell surface recycling pathway toward late endocytic compartments for degradation (Poirier and Mayer, 2013). In a previous study, we have identified annexin A2 as an endogenous PCSK9-binding protein and extrahepatic inhibitor of PCSK9-enhanced LDLR degradation (Mayer et al., 2008; Seidah et al., 2012). So far, no other such endogenous PCSK9 inhibitor has been identified at the cell surface or within the secretory pathway of hepatocytes.

Under physiological or stress conditions, the ER tightly maintains cellular integrity through the help of crucial factors such as calnexin, calreticulin, glucose-regulated protein 78 (GRP78), GRP94, and PDIs (Ni and Lee, 2007). GRP94, also known as gp96, is a highly abundant ER-resident protein recognized primarily as a luminal molecular chaperone but also as a potent calcium- and peptide-binding protein (Lee, 2014). Unlike GRP78, functional studies revealed that folding and secretion of a very restrictive number of client proteins were solely dependent on GRP94 (Marzec et al., 2012). In addition, folding of particular proteins can be driven by private chaperones. Indeed, Boca/Mesd (Culi and Mann, 2003) and receptor-associated protein (RAP) (Bu et al., 1995) were identified as specific molecular chaperones for LDLR family members that allow for their proper folding and prevent early interaction with their ligands within the secretory pathway.

Whereas the liver is by far the richest source of PCSK9, it remains intriguing why hepatic LDLR remains abundant and not completely degraded by PCSK9. Therefore, we hypothesized that PCSK9 interacts with one or more yet unidentified protein(s) to prevent early LDLR binding and degradation under physiological conditions.

RESULTS AND DISCUSSION

Identification of GRP94 as an Endogenous PCSK9-Binding Protein

To identify interacting proteins, PCSK9 was immunoprecipitated (IP) under both physiological (Figure 1A) or overexpressed

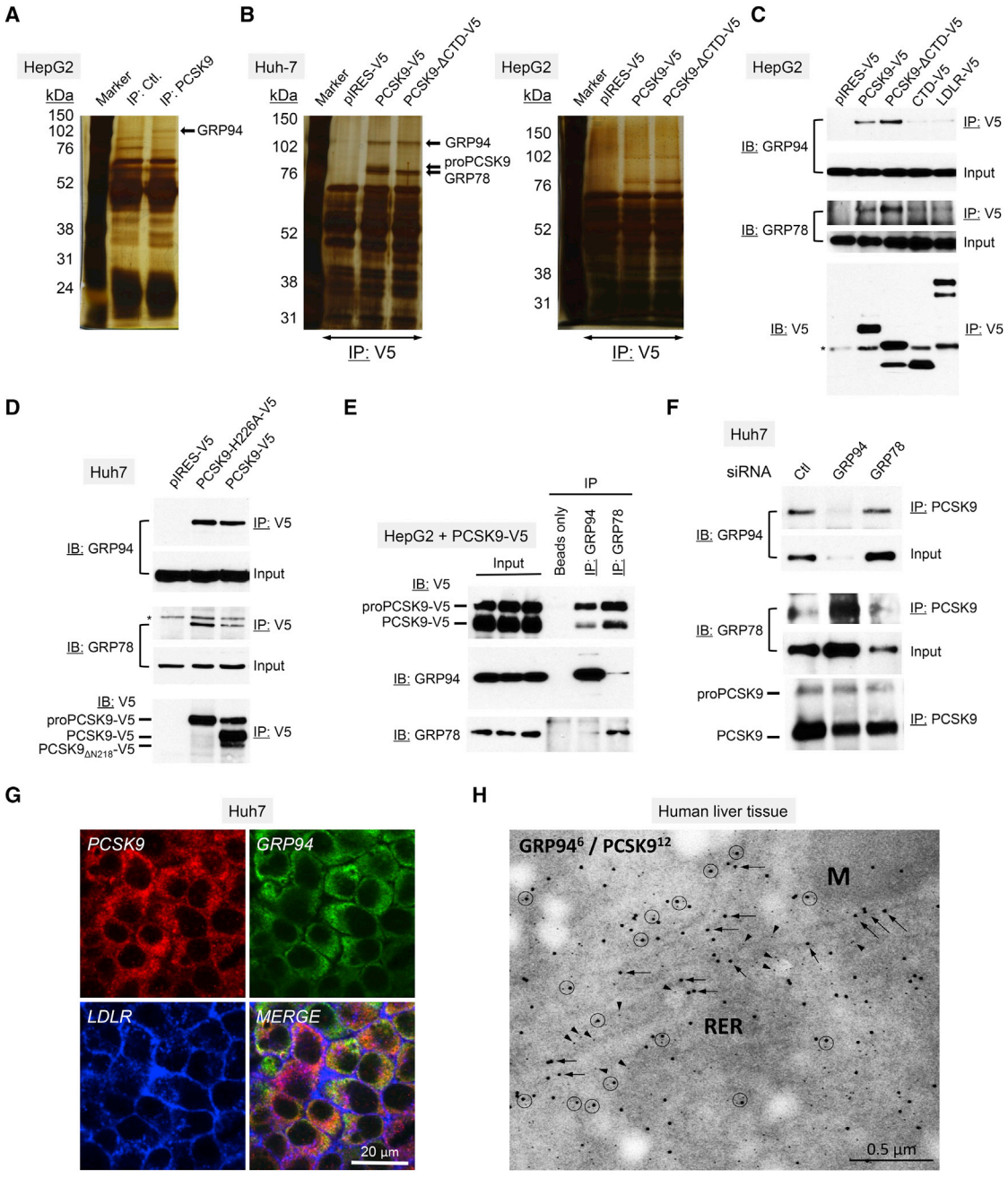

Figure 1. Identification of PCSK9-Interacting Proteins

(A and B) Silver staining of proteins immunoprecipitated (IP) with endogenous PCSK9 from HepG2 cells (A) or with overexpressed V5-tagged PCSK9 or PCSK9-ΔCTD-V5 from HepG2 or Huh-7 cells (B). Indicated proteins (arrows) were identified by mass spectrometry (see also Figure S1).

(C–E) Immunoblots (IBs) showing coIP of endogenous GRP94 or GRP78 with PCSK9 and mutants thereof from HepG2 or Huh-7 cells transfected with V5-tagged constructs, as indicated. Asterisks indicate non-specific bands.

(F) IB showing coIP of endogenous PCSK9 with GRP94 or GRP78 from Huh-7 cells transfected with siRNAs against GRP94 or GRP78.

(G) Confocal immunofluorescence microscopy of endogenous PCSK9, GRP94, and LDLR in Huh-7 cells.

(H) Double immunogold localization of GRP94 (6-nm gold particles, arrowheads) and PCSK9 (12-nm gold particles, arrows) in normal human liver tissue. Colocalization events (encircled) in the rough ER (RER) are emphasized (see also Figure S2).

Data are representative of at least three independent experiments.

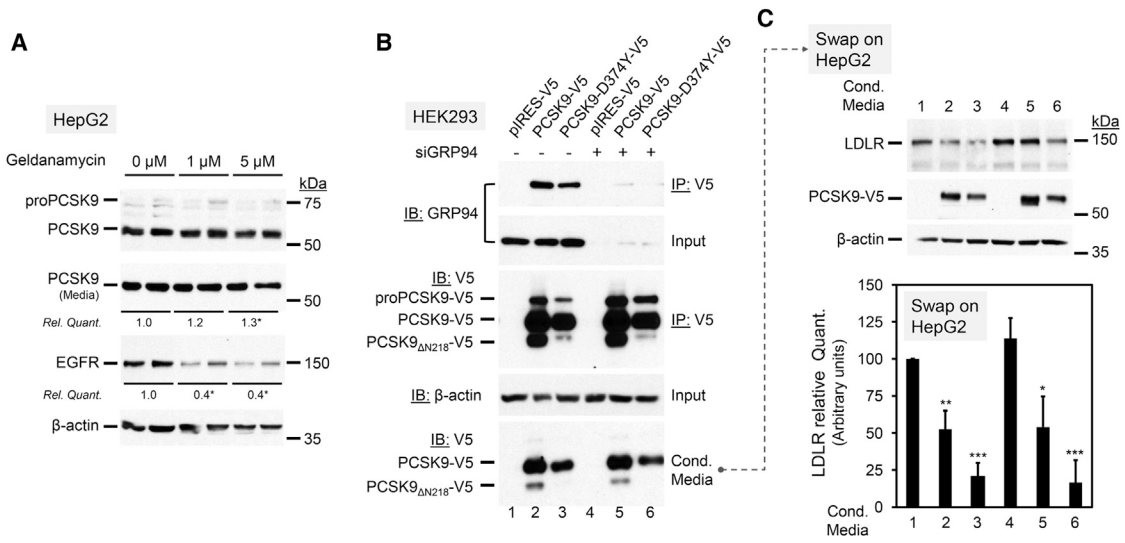

Figure 2. GRP94 Is Not an Obligatory Chaperone for PCSK9

(A) HepG2 cells were incubated for 18 hr with 0 (DMSO), 1, or 5 μM geldanamycin. PCSK9 (lysates and conditioned media) and EGFR (positive control for geldanamycin) protein levels were analyzed by IB, quantified and normalized over β-actin.

(B) IP of overexpressed PCSK9-V5 or its D374Y mutant from cell lysates of HEK293 cells transfected either with non-targeting siRNAs (−) or with siGRP94 (+) and analyzed by IB as indicated.

(C) HepG2 cells were incubated for 18 hr with conditioned media derived from HEK293 cells prepared in (B) (dotted line) and analyzed by IB as indicated. LDLR levels were quantified and normalized over β-actin (bottom panel).

Data are representative of at least three to four independent experiments. Bars and data from gel quantifications are means ± SD. *$p < 0.05$; **$p < 0.01$; ***$p < 0.001$.

(Figure 1B) conditions from human hepatic HepG2 or Huh-7 cells. Co-interacting proteins were separated by SDS-PAGE and highlighted by silver staining. Mass spectrometry data from the excised bands revealed human GRP94 as the major ~100-kDa migrating protein in complex with PCSK9 in both conditions (Figures 1A, 1B, S1A, and S1B). The analysis also revealed GRP78 as the major ~76-kDa protein interacting with overexpressed PCSK9-V5 together with the uncleaved proPCSK9 precursor present in the ER (Figures 1B and S1B). Independently of its C-terminal Cys/His-rich domain (CTD or CHRD), immunoblotting confirmed that PCSK9-V5, but not LDLR-V5, specifically interacts in complex with GRP94 and GRP78 (Figure 1C). GRP94 and GRP78 also interacted with the catalytically inactive PCSK9-H226A-V5 mutant (Figure 1D) retained in the ER (Seidah et al., 2003). However, both proPCSK9-V5 and mature PCSK9-V5 were IP using either anti-GRP94 or anti-GRP78 (Figure 1E), suggesting that the interaction of PCSK9 with those chaperones might not be exclusively linked to zymogen activation and/or folding of PCSK9 during de novo synthesis.

As previously reported (Jansen et al., 2012), we observed a slight interaction between GRP94 and GRP78 (Figure 1E). To delineate the interdependence of GRP78 and GRP94 in PCSK9 complex formation, PCSK9 was IP following siRNA-mediated knockdown (KD) of GRP78 or GRP94 (Figure 1F). The data showed that endogenous GRP78 interacted with PCSK9 only upon GRP94 KD and that GRP78 is not an intermediate in the PCSK9-GRP94 complex formation (Figure 1F; siGRP78). In agreement with coIP experiments, endogenous PCSK9 and GRP94, but not LDLR, co-localized in Huh-7 cells (Figure 1G) and were found associated in the ER of normal human hepatocytes (Figures 1H and S2), supporting their interaction in physiological conditions. As compared to GRP94, GRP78 has a wide variety of client proteins and plays pivotal roles in the unfolded protein response associated to ER stress in addition to being an anti-apoptotic and pro-proliferative regulator (Lee, 2014). Indeed, the absence of GRP94 did not affect cell viability or the general expression of surface protein in isolated mammalian cells (Randow and Seed, 2001). At this point of the study, we consequently decided to focus our work on the specific role of GRP94 on PCSK9 based on the above identification of hepatic GRP94 as an endogenous PCSK9 intracellular binding protein.

GRP94 Is Not an Essential Molecular Chaperone for PCSK9

Next, we wanted to determine whether GRP94 is required for PCSK9 synthesis and processing by treating HepG2 cells with geldanamycin (GA), a small molecule competitive inhibitor of the N-terminal ATP-binding site of GRP94 (Stebbins et al., 1997). Whereas GA affects EGFR levels (Supino-Rosin et al., 2000), it did not perturb intracellular proPCSK9 to PCSK9 autocatalytic activation and PCSK9 secretion (Figure 2A), suggesting that GRP94 activity is dispensable for PCSK9 processing. To further substantiate these observations, HEK293 cells were transfected with siRNAs against human GRP94 together with PCSK9-V5 or its high LDLR affinity gain-of-function D374Y mutant (Figure 2B; reviewed in Poirier and Mayer, 2013). Both WT and PCSK9-D374Y mutant similarly and specifically

interacted with GRP94 as clearly demonstrated following KD of GRP94 (Figure 2B; *IP*:*V5*; *IB*:*GRP94*). Consistent with enzymatic inhibition of GRP94 (Figure 2A), KD of GRP94 did not alter PCSK9 protein levels, autocatalytic cleavage, furin-regulated processing (PCSK9-ΔN_{218}; Benjannet et al., 2006), or its secretion (Figure 2B; Cond. Media), and PCSK9 maintained its full capacity to induce LDLR degradation following media swap on naive HepG2 cells (Figure 2C). Therefore, we conclude that GRP94 is not an essential chaperone for PCSK9 in immortalized mammalian cells.

Hepatic GRP94 Controls Circulating LDLc by Maintaining LDLR Protein Levels

Hepatocytes regulate clearance of plasma LDLc via cell surface LDLR in addition to being the main cell type expressing PCSK9 (Goldstein and Brown, 1987; Seidah et al., 2003). Accordingly, floxed-*Grp94* mice were crossed with albumin-Cre transgenic mice to generate hepatocyte-specific *Grp94*-deficient mice (*cGrp94f/f* mice; Chen et al., 2014). Similar to *Ldlr*-deficient mice (Poirier et al., 2009), circulating PCSK9 levels were elevated in the plasma of *cGrp94f/f* mice (Figure 3A), which substantiate in vivo that GRP94 is not an obligatory chaperone for PCSK9 processing and secretion by hepatocytes. In parallel, we also observed a 14-fold increase in circulating LDLc in *cGrp94f/f* mice (Figure 3A, bottom panel). Whereas *Ldlr* mRNA expression was not affected (not shown), LDLR protein levels were severely decreased in livers of *cGrp94f/f* mice (Figure 3B), reminiscent of PCSK9 overexpression phenotype (Maxwell and Breslow, 2004). Importantly, we did not observe any significant difference for other cell surface transmembrane proteins such as P-cadherin and CD36 in livers of *cGrp94f/f* mice (Figure 3B), demonstrating that GRP94 regulates LDLc by modulating LDLR protein levels.

GRP94 Protects LDLR from PCSK9-Induced Degradation

Next, we questioned whether the observed effect on LDLR could be related to ER stress or calcium disturbance as GRP94 is a calcium-binding protein and has been functionally correlated with the unfolded protein response (Ni and Lee, 2007). Overnight treatment with thapsigargin (TG), a sarco/ER Ca^2-ATPase inhibitor and ER stress inducer, in HEK293 cells or mouse embryonic fibroblasts (MEFs) significantly reduced LDLR levels (Figures 3C and 3D) without affecting overexpressed PCSK9 processing and secretion (Figure 3C). In contrast, GRP94 KD did not affect intracellular ER Ca^{2+} homeostasis (Figure 3E) and did not alter LDLR protein levels in naturally PCSK9-deficient HEK293 cells (Seidah et al., 2003; Figure 3F) as compared to PCSK9-rich hepatocytes of *cGrp94f/f* mice (Figures 3B and 3D). Moreover, whereas TG induced expression of GRP78 and ER stress marker CHOP in MEFs, a mild compensatory increase in GRP78 (Chen et al., 2014) but no activation of ER stress were observed in livers of *cGrp94f/f* (Figure 3D). Together, these data imply a direct involvement of PCSK9 rather than chaperoning or calcium-buffering effects of GRP94 on LDLR.

To test whether GRP94 is required to maintain LDLR protein levels in the presence of PCSK9, HepG2 cells were transfected with cDNA constructs encoding PCSK9-mCherry and LDLR-EGFP. As shown in Figure 3G, LDLR-EGFP is well expressed at the cell surface and co-localized with PCSK9-D374Y-mCherry (Figure 3H, left panels), the latter preserving its capacity to induce LDLR degradation (Figure 3H, right panels). Interestingly, KD of GRP94 rendered LDLR much more sensitive to PCSK9-induced degradation (Figure 3I, lane 5 and right top panel). Moreover, the proteasome inhibitor MG132 did not block PCSK9-induced LDLR degradation following KD of GRP94, eliminating rerouting of the PCSK9/LDLR complex to the ER-associated degradation pathway (Figure 3I, lane 6 and right bottom). Therefore, GRP94 could prevent PCSK9 binding to LDLR and thus limit its subsequent degradation.

Inhibitory Effects of GRP94-CBD-CT Domain on PCSK9-Induced LDLR Degradation

It was reported that a 27-aa C-terminal hydrophobic loop structure within the GRP94 client-binding domain (CBD) (aa 652–678; Figure 4A) is important for folding and interaction with Toll-like receptors and integrins (Wu et al., 2012). Deletion or alanine-scan mutations in the CBD of GRP94 did not alter its overall structure or its ATPase activity but prevented interaction with its client proteins (Wu et al., 2012). Similarly, we generated secretable HA-tagged cDNA constructs of human GRP94, lacking its ER-retention C-terminal KDEL sequence, in which critical CBD residues were mutated to alanine (AA1 and AA2, highlighted in blue and red, respectively; Figure 4B). Although expressed at similar levels to WT, mutations within CBD domain (AA1 or AA2) abrogated binding to PCSK9 (Figure 4B). Next, we truncated the whole N-terminal enzymatic domain, resulting in a small secretable ~20-kDa protein encoding the CBD and CT domains sufficient for interaction with client proteins (Wu et al., 2012). Whereas the CBD-CT construct was ~5-fold less produced and secreted by HEK293 cells, its interaction with PCSK9 was significantly enhanced as compared to full-length (FL) GRP94 (Figure 4C), reinforcing the major role of CBD for GRP94-PCSK9 interaction.

Next, we used purified or secretable GRP94 or its CBD-CT domain as surrogates to intracellular GRP94 to test directly for the inhibition of PCSK9. Confocal microscopy revealed that PCSK9-mCherry endocytosis was significantly reduced in LDLR-EGFP-expressing cells in the presence of recombinant GRP94 (Figure 4D). Although HepG2 cells secrete a small amount of endogenous GRP94 (~5 nM; Figure 4E, lane 1; Mangrum et al., 2015), immunoblot data revealed that PCSK9-induced LDLR degradation was reversed in a dose-dependent manner by addition of GRP94 (Figure 4E, lanes 2–6). These data demonstrate that exogenous GRP94 efficiently inhibits PCSK9-induced LDLR degradation likely by blocking PCSK9 interaction and LDLR-mediated internalization and also suggest that GRP94 could block the PCSK9-LDLR interaction in the ER. In accordance with apparent increased affinity of PCSK9 for CBD-CT as compared to FL GRP94 (Figure 4C), PCSK9 and CBD-CT were completely co-localized in a diffuse structure reminiscent of the ER (Figure 4F, solid arrows) and in the perinuclear *Golgi*-like compartment (Figure 4F, dashed arrows), whereas PCSK9 and FL GRP94 mainly co-localized in the ER-like compartment. Similar to recombinant GRP94 (Figure 4E), overexpression of secretable FL GRP94 or CBD-CT significantly blocked LDLR degradation induced by PCSK9 in Huh-7 (Figure 4G) and

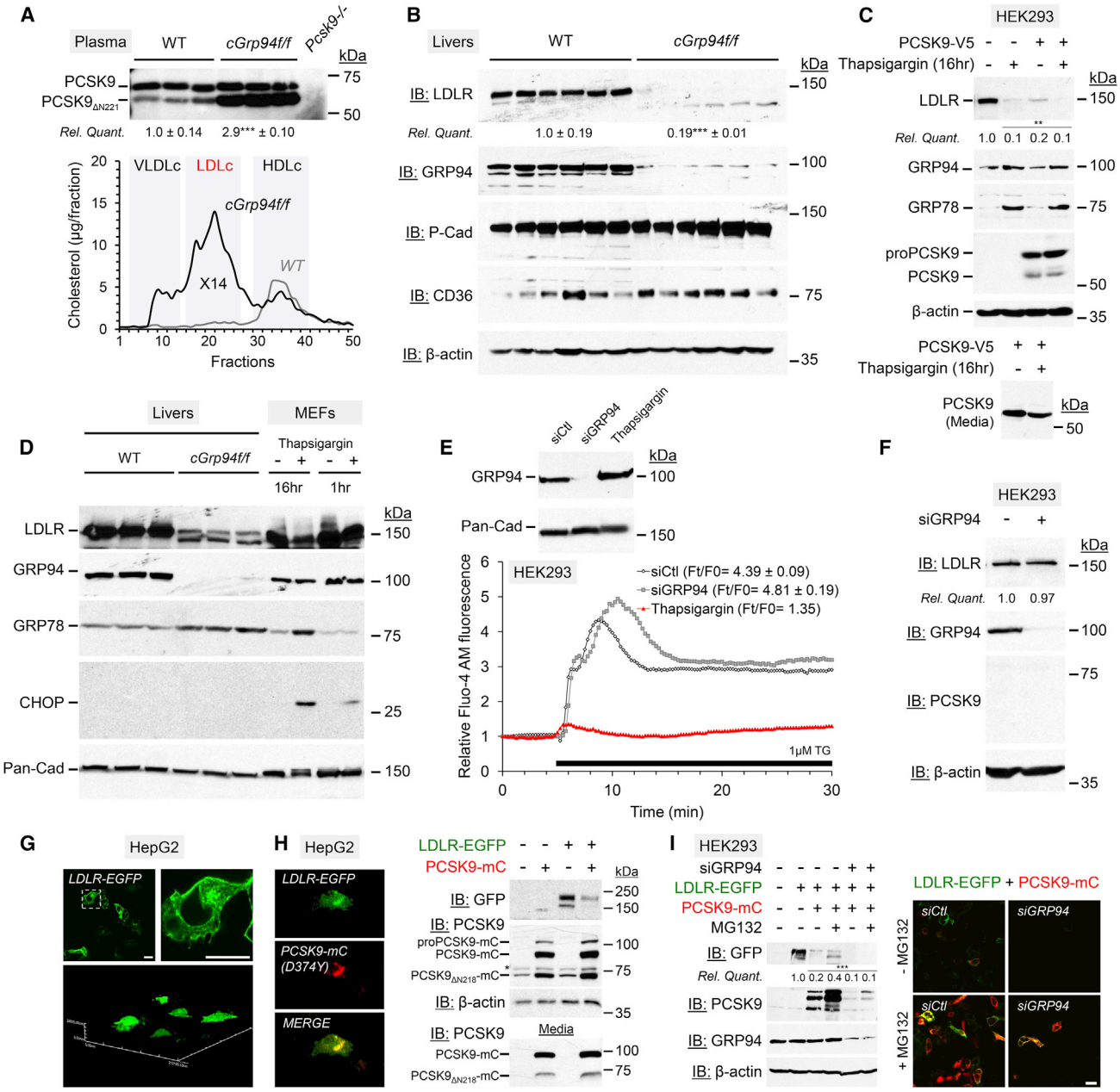

Figure 3. Absence of GRP94 Increases LDLR Degradation by PCSK9

(A) Plasma PCSK9 levels (top panel; *Pcsk9*$^{-/-}$ plasma; negative control) and lipoprotein cholesterol profiles (bottom panel) from WT and *cGrp94f/f* mice were analyzed as described in Supplemental Experimental Procedures.

(B) IB analysis of hepatic LDLR, GRP94, P-cadherin, CD36, and β-actin in WT and *cGrp94*$^{f/f}$ mice.

(C) IB of thapsigargin-treated (16 hr) HEK293 cells transfected without (–) or with PCSK9-V5.

(D) IB of LDLR, GRP94, GRP78, CHOP, and P-cadherin in WT and *cGrp94*$^{f/f}$ mice and thapsigargin-treated (1 or 16 hr) MEFs.

(E and F) Thapsigargin-sensitive Ca^{2+} stores were monitored by live-cell confocal microscopy, and proteins were analyzed by IB in HEK293 cells transfected with non-targeting siRNAs (–) or siGRP94 (+) or treated with thapsigargin (16 hr; herein used as ER Ca^{2+}-depleted condition) as indicated.

(G–I) Confocal microscopy of intracellular (G, top panels) and cell surface LDLR-EGFP (z stack reconstruction shown in G, lower panel) and its co-localization with PCSK9-mCherry (PCSK9-mC; H) in HepG2 cells under basal conditions or following transfection with either non-targeting siRNAs (–) or with siGRP94 (+) in the absence (–) or presence of MG132 in HEK293 cells (I, right panels). The scale bars represent 20 µm. Corresponding total protein levels were analyzed by IB as indicated (H, right panels, and I, left panels).

All data are representative of at least three independent experiments. Data are means ± SD. **p < 0.01; ***p < 0.001.

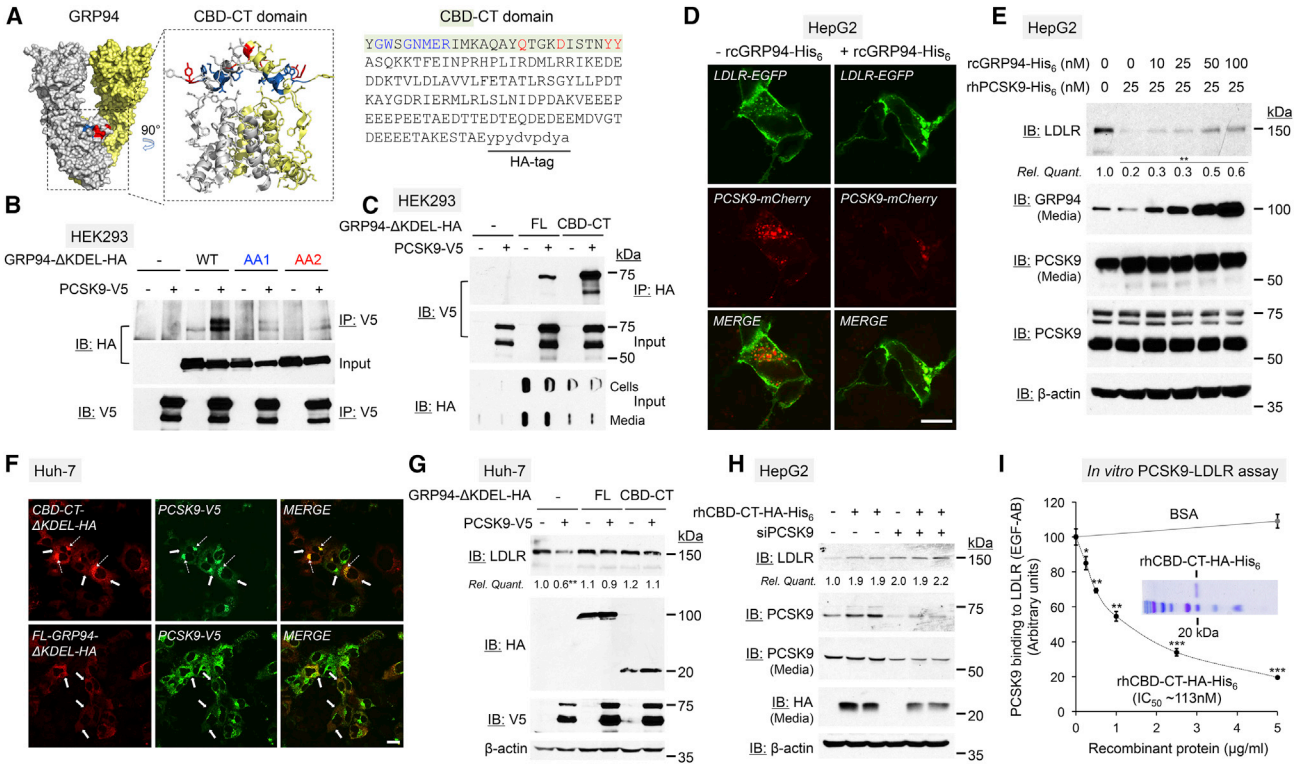

Figure 4. GRP94-CBD-CT Domain Inhibits PCSK9-Induced LDLR Degradation

(A–C) Mapping of the PCSK9-GRP94-interacting domain. GRP94 structure was extracted from PDB: 2O1V using MacPymol software, and the CBD-CT domain is emphasized (A, middle and right panels). IP of PCSK9-V5 from HEK293 cells co-transfected without (–) or with GRP94-ΔKDEL-HA (B and C), its alanine scanning mutants (AA1, blue, or AA2, red; B), or its CBD-CT domain (C) was analyzed by IB as indicated. Data are representative of at least three independent experiments.

(D) Internalization of PCSK9-mCherry in LDLR-EGFP-expressing HepG2 cells in the absence or presence of recombinant GRP94 was analyzed by confocal microscopy. The scale bar represents 20 μm. Data are representative of at least three independent experiments.

(E) HepG2 cells were incubated overnight without or with recombinant PCSK9 together with increasing concentrations of recombinant GRP94. Protein levels in cells and media were analyzed by IB as indicated. Data are representative of at least three independent experiments.

(F and G) Huh-7 cells were transfected without or with PCSK9-V5, full-length GRP94-ΔKDEL-HA (FL), or its CBD-CT domain. Subcellular localization was visualized by confocal microscopy (F; scale bar, 20 μm), and protein levels were analyzed by IB, as indicated (G). Data are representative of at least three independent experiments.

(H) HepG2 cells were transfected with non-targeting siRNAs (–) or siPCSK9 for 48 hr and incubated 18 hr with 2 μg/ml recombinant CBD-CT-HA-His_6. Protein levels in lysates and media were analyzed by IB as indicated. Data were analyzed in duplicate.

(I) The inhibitory effect of rhCBD-CT-HA-His_6 on PCSK9-LDLR (EGF-AB) binding was analyzed by in vitro competitive assay. Coomassie staining of rhCBD-CT-HA-His_6 is shown. Data represent means of two independent experiments analyzed in duplicate ± SD. *$p < 0.05$; **$p < 0.01$; ***$p < 0.001$.

Data from gel quantifications (normalized over β-actin; E, G, and H) are means ± SD. **$p < 0.01$.

HepG2 cells (data not shown). Furthermore, addition of recombinant CBD-CT significantly increased total LDLR protein levels in a PCSK9-dependent manner (Figure 4H), most likely via a direct competition with LDLR-EGF-A domain for PCSK9 (Figure 4I). Overall, these data demonstrated that PCSK9-GRP94 complex formation, and more specifically its CDB-CT domain, has a direct inhibitory effect on the binding of PCSK9 to LDLR and its subsequent degradation.

Indicative of its very restrictive selection of client proteins, tissue- or cell-type targeted deletions of *Grp94* have underlined its specific roles in the maintenance of organ homeostasis, innate and adaptive immunity, and cancer progression (Lee, 2014). In the present study, we identified GRP94 as an ER-resident PCSK9-interacting protein (Figures 1A, 1G, and 1H) and inhibitor of PCSK9-LDLR complex formation (Figure 4I). Accordingly, hepatocyte-specific deletion of *Grp94* severely increased plasma PCSK9 and LDLc levels (Figure 3A), which is correlated with almost undetectable hepatic LDLR protein levels (Figure 3B). Moreover, we showed that LDLR was much more sensitive to degradation in the absence of GRP94 in PCSK9-expressing cells and liver (Figures 3B, 3I, and 4G). As a physiological mechanism, we propose that GRP94 regulates circulating LDLc and sustains LDLR protein levels likely by preventing PCSK9-LDLR binding in the ER of hepatocytes.

We previously identified annexin A2 as an endogenous PCSK9-CTD-binding protein and potent extrahepatic inhibitor of PCSK9-mediated LDLR degradation (Mayer et al., 2008; Seidah et al., 2012). In contrast, GRP94 is highly expressed in hepatocytes and its interaction with PCSK9 involves the catalytic domain and directly competes for binding with LDLR-EGF-A

domain (Figure 4I). Molecular characterization revealed that GRP94 is not an obligatory chaperone for PCSK9 and that, unlike CBD domain, the GRP94 N-terminal domain, important for folding of its client proteins, is not involved in PCSK9 interaction and subsequent inhibition of LDLR degradation. In terms of functional therapeutics, one may think that the presence of GRP94, or preferably CBD-CT or CBD that lacks its chaperoning domain, in the plasma would not interfere with the physiological functions of GRP94 normally occurring in the ER. Therefore, as demonstrated in this study, GRP94 and fragments thereof may be used therapeutically to target PCSK9 and block binding to LDLR, preventing its intracellular degradation and, hence, reducing LDLc and the risk of CHD.

EXPERIMENTAL PROCEDURES

A detailed description of all methods can be found in the Supplemental Experimental Procedures. All animal studies were approved by the University of Southern California Institutional Animal Care and Use Committee and the Montreal Heart Institute Animal Care and Ethical Committee. Hepatocyte-specific *Grp94*-deficient male mice (*cGrp94f/f*) were obtained by crossing Alb-Cre with *Grp94f/f* mice (Chen et al., 2014). Littermates lacking Alb-Cre served as WT controls. Blood samples were collected by cardiac puncture, and livers were dissected and snap frozen in liquid nitrogen for further analyses as indicated. Cell culture, plasmid constructions, and transfections were performed according to standard protocols as described in the Supplemental Experimental Procedures. For IP, cells were lysed in RIPA buffer without or with SDS and V5 or HA-tagged proteins, PCSK9, GRP94, or GRP78 were immunoprecipitated with indicated antibodies. PCSK9-interacting proteins were identified by mass spectrometry. For western blot analyses, cells and tissue samples were lysed in RIPA buffer and proteins were separated by SDS-PAGE, transferred to nitrocellulose membranes, and incubated with indicated antibodies. Human PCSK9 was obtained from conditioned media of HEK293T transiently transfected with His_6-tagged PCSK9. GRP94-CDB-CT-ΔKDEL-HA-His_6 was produced following IPTG induction in T7 competent *E. coli* and recovered from bacterial lysates. Both proteins were purified by affinity followed by size exclusion chromatography and used for cell-based PCSK9 competitive assays. Solid phase PCSK9-LDLR(EGF-AB) in vitro competitive binding assay (Circulex; cat. no. CY-8150) with recombinant CBD-CT-HA-His_6 was performed according to manufacturer's recommendations. All data are presented as mean ± SD and are representative of at least three independent experiments analyzed in duplicate. Protein bands from SDS-PAGE were quantified and normalized using GelEval software. Statistical analysis was performed using Student's t test. $p < 0.05$ was considered statistically significant.

SUPPLEMENTAL INFORMATION

Supplemental Information includes Supplemental Experimental Procedures, two figures, and one table and can be found with this article online at http://dx.doi.org/10.1016/j.celrep.2015.11.006.

AUTHOR CONTRIBUTIONS

S.P. designed, performed, interpreted the results, and wrote the manuscript. M.M. helped in generating cDNA constructs. W.-T.C. and A.S.L. provided samples from the *cGrp94f/f* and WT control littermates and revised the manuscript. G.M. designed, interpreted the results, and wrote the manuscript.

ACKNOWLEDGMENTS

We thank Denis Faubert (IRCM) for excellent support with LC-MS/MS analyses and Dat Ha and Jieli Shen (USC) for assistance with mouse tissues. We are grateful to our colleagues at the MHI for expert advice regarding production of recombinant proteins (Dr. Bruce Allen), intracellular calcium dynamics experimental design (Dr. Jonathan Ledoux), and live-cell data acquisition (Louis Villeneuve). A.S.L. is funded by the NIH grant CA-027607. G.M. is funded by the Canadian Institutes of Health Research grant MOP133598, the Heart and Stroke Foundation of Canada, the Fonds de recherche Québec-Santé, and the Montreal Heart Institute Foundation.

Received: May 11, 2015
Revised: October 12, 2015
Accepted: October 31, 2015
Published: November 25, 2015

REFERENCES

Abifadel, M., Varret, M., Rabès, J.P., Allard, D., Ouguerram, K., Devillers, M., Cruaud, C., Benjannet, S., Wickham, L., Erlich, D., et al. (2003). Mutations in PCSK9 cause autosomal dominant hypercholesterolemia. Nat. Genet. *34*, 154–156.

Benjannet, S., Rhainds, D., Hamelin, J., Nassoury, N., and Seidah, N.G. (2006). The proprotein convertase (PC) PCSK9 is inactivated by furin and/or PC5/6A: functional consequences of natural mutations and post-translational modifications. J. Biol. Chem. *281*, 30561–30572.

Bu, G., Geuze, H.J., Strous, G.J., and Schwartz, A.L. (1995). 39 kDa receptor-associated protein is an ER resident protein and molecular chaperone for LDL receptor-related protein. EMBO J. *14*, 2269–2280.

Chen, W.T., Tseng, C.C., Pfaffenbach, K., Kanel, G., Luo, B., Stiles, B.L., and Lee, A.S. (2014). Liver-specific knockout of GRP94 in mice disrupts cell adhesion, activates liver progenitor cells, and accelerates liver tumorigenesis. Hepatology *59*, 947–957.

Cohen, J., Pertsemlidis, A., Kotowski, I.K., Graham, R., Garcia, C.K., and Hobbs, H.H. (2005). Low LDL cholesterol in individuals of African descent resulting from frequent nonsense mutations in PCSK9. Nat. Genet. *37*, 161–165.

Culi, J., and Mann, R.S. (2003). Boca, an endoplasmic reticulum protein required for wingless signaling and trafficking of LDL receptor family members in Drosophila. Cell *112*, 343–354.

Cunningham, D., Danley, D.E., Geoghegan, K.F., Griffor, M.C., Hawkins, J.L., Subashi, T.A., Varghese, A.H., Ammirati, M.J., Culp, J.S., Hoth, L.R., et al. (2007). Structural and biophysical studies of PCSK9 and its mutants linked to familial hypercholesterolemia. Nat. Struct. Mol. Biol. *14*, 413–419.

Goldstein, J.L., and Brown, M.S. (1987). Regulation of low-density lipoprotein receptors: implications for pathogenesis and therapy of hypercholesterolemia and atherosclerosis. Circulation *76*, 504–507.

Jansen, G., Määttänen, P., Denisov, A.Y., Scarffe, L., Schade, B., Balghi, H., Dejgaard, K., Chen, L.Y., Muller, W.J., Gehring, K., and Thomas, D.Y. (2012). An interaction map of endoplasmic reticulum chaperones and foldases. Mol. Cell. Proteomics *11*, 710–723.

Lee, A.S. (2014). Glucose-regulated proteins in cancer: molecular mechanisms and therapeutic potential. Nat. Rev. Cancer *14*, 263–276.

Mangrum, J.B., Martin, E.J., Brophy, D.F., and Hawkridge, A.M. (2015). Intact stable isotope labeled plasma proteins from the SILAC-labeled HepG2 secretome. Proteomics *15*, 3104–3115.

Marzec, M., Eletto, D., and Argon, Y. (2012). GRP94: An HSP90-like protein specialized for protein folding and quality control in the endoplasmic reticulum. Biochim. Biophys. Acta *1823*, 774–787.

Maxwell, K.N., and Breslow, J.L. (2004). Adenoviral-mediated expression of Pcsk9 in mice results in a low-density lipoprotein receptor knockout phenotype. Proc. Natl. Acad. Sci. USA *101*, 7100–7105.

Maxwell, K.N., Soccio, R.E., Duncan, E.M., Sehayek, E., and Breslow, J.L. (2003). Novel putative SREBP and LXR target genes identified by microarray analysis in liver of cholesterol-fed mice. J. Lipid Res. *44*, 2109–2119.

Mayer, G., Poirier, S., and Seidah, N.G. (2008). Annexin A2 is a C-terminal PCSK9-binding protein that regulates endogenous low density lipoprotein receptor levels. J. Biol. Chem. *283*, 31791–31801.

McNutt, M.C., Lagace, T.A., and Horton, J.D. (2007). Catalytic activity is not required for secreted PCSK9 to reduce low density lipoprotein receptors in HepG2 cells. J. Biol. Chem. *282*, 20799–20803.

Ni, M., and Lee, A.S. (2007). ER chaperones in mammalian development and human diseases. FEBS Lett. *581*, 3641–3651.

Nordestgaard, B.G., Chapman, M.J., Humphries, S.E., Ginsberg, H.N., Masana, L., Descamps, O.S., Wiklund, O., Hegele, R.A., Raal, F.J., Defesche, J.C., et al.; European Atherosclerosis Society Consensus Panel (2013). Familial hypercholesterolaemia is underdiagnosed and undertreated in the general population: guidance for clinicians to prevent coronary heart disease: consensus statement of the European Atherosclerosis Society. Eur. Heart J. *34*, 3478–3490.

Poirier, S., and Mayer, G. (2013). The biology of PCSK9 from the endoplasmic reticulum to lysosomes: new and emerging therapeutics to control low-density lipoprotein cholesterol. Drug Des. Devel. Ther. *7*, 1135–1148.

Poirier, S., Mayer, G., Poupon, V., McPherson, P.S., Desjardins, R., Ly, K., Asselin, M.C., Day, R., Duclos, F.J., Witmer, M., et al. (2009). Dissection of the endogenous cellular pathways of PCSK9-induced low density lipoprotein receptor degradation: evidence for an intracellular route. J. Biol. Chem. *284*, 28856–28864.

Randow, F., and Seed, B. (2001). Endoplasmic reticulum chaperone gp96 is required for innate immunity but not cell viability. Nat. Cell Biol. *3*, 891–896.

Seidah, N.G., Benjannet, S., Wickham, L., Marcinkiewicz, J., Jasmin, S.B., Stifani, S., Basak, A., Prat, A., and Chretien, M. (2003). The secretory proprotein convertase neural apoptosis-regulated convertase 1 (NARC-1): liver regeneration and neuronal differentiation. Proc. Natl. Acad. Sci. USA *100*, 928–933.

Seidah, N.G., Poirier, S., Denis, M., Parker, R., Miao, B., Mapelli, C., Prat, A., Wassef, H., Davignon, J., Hajjar, K.A., and Mayer, G. (2012). Annexin A2 is a natural extrahepatic inhibitor of the PCSK9-induced LDL receptor degradation. PLoS ONE *7*, e41865.

Stebbins, C.E., Russo, A.A., Schneider, C., Rosen, N., Hartl, F.U., and Pavletich, N.P. (1997). Crystal structure of an Hsp90-geldanamycin complex: targeting of a protein chaperone by an antitumor agent. Cell *89*, 239–250.

Supino-Rosin, L., Yoshimura, A., Yarden, Y., Elazar, Z., and Neumann, D. (2000). Intracellular retention and degradation of the epidermal growth factor receptor, two distinct processes mediated by benzoquinone ansamycins. J. Biol. Chem. *275*, 21850–21855.

Wu, S., Hong, F., Gewirth, D., Guo, B., Liu, B., and Li, Z. (2012). The molecular chaperone gp96/GRP94 interacts with Toll-like receptors and integrins via its C-terminal hydrophobic domain. J. Biol. Chem. *287*, 6735–6742.